Computed Energy Density and Surface Energy of a Fermi Gas in a Cubical Box

Ansh R. Gupta [ID][1]

[1] *Steward Observatory, University of Arizona, 933 N Cherry Avenue, Tucson, AZ 85721, USA*

1. INTRODUCTION

Fermions are particles with a half-integer spin, such as $\frac{1}{2}$, $\frac{3}{2}$, etc. Unlike bosons, they obey the Pauli exclusion principle, meaning that two fermions cannot occupy the same quantum state. This fact results in many of the characteristics and properties of a "Fermi gas" at low temperatures and/or high densities, when quantum effects are not negligible (Fermi 1926). Under these extreme conditions, the wavefunctions of the constituent particles of a Fermi gas experience significant overlap. The exclusion principle then generates a "Fermi pressure" which resists compression (Fowler 1926)(Dyson & Lenard 1967). This, for example, is responsible for preventing the collapse of white dwarf stars (Stoner 1930)(Chandrasekhar 1931). Analysis of a non-interacting ideal fermion gas can also be applied to describe the behavior of free electrons in metals (Sommerfeld 1928) and supercooled liquid ^{3}He (Schulz 1995).

2. PROJECT DESCRIPTION

Consider a system of fermions in a 3 dimensional, cubical box with side length L. Analytically, the expected relationship between the side length of the box and the average energy of the system can be found in terms of the volume of the box (V), its surface area (A), a small fluctuating term (δE) (Stafford et al. 1999).

$$E = \rho_E V + \sigma_E A + \delta E \qquad (1)$$

Here, I reproduce this relationship by calculating the average total energy of a Fermi gas for a variety of box side lengths. The analysis is carried out for multiple regimes of temperatures and chemical potentials. By fitting the analytical form of the relationship to the computed values, the energy density of the Fermi gas ρ_E, surface energy σ_E, and fluctuation term δE are found.

3. THEORY

A system of ideal, non-interacting fermions in a cubical container can be treated to a good approximation as a collection of quantum particles in a 3D box. The energy eigenvalues for an individual fermion can be found as

$$\epsilon_{\vec{n}} = \frac{\pi^2 \hbar^2 \vec{n}^2}{2mL^2} \qquad (2)$$

where m is the particle mass. A treatment of this problem can be found in many introductory quantum mechanics textbooks (Griffiths & Schroeter 2018). 3 quantum numbers, n_x, n_y, and n_z, must be introduced to express the allowed energy eigenvalues for a particle in a 3D box. Then the quantity $\vec{n}^2 = n_x^2 + n_y^2 + n_z^2$.

A statistical mechanical analysis can be used to find the probability of a state with a particular energy ϵ being occupied at a given temperature and chemical potential (Hoch 2021). The resulting probability function is known as the Fermi-Dirac (FD) distribution, named after physicists Enrico Fermi and Paul Dirac. The FD distribution is found to be

$$f_+ = \frac{1}{e^{\beta(\epsilon - \mu)} + 1} \qquad (3)$$

Where β is the *thermodynamic beta* ($\frac{1}{k_B T}$) and μ is the chemical potential of the system. Conducting a summation of the FD distribution over all possible combinations of quantum numbers yields the average total number of particles of the system.

$$N = \sum_{n_x} \sum_{n_y} \sum_{n_z} f_+(\epsilon) \qquad (4)$$

Similarly, the average total energy of the system can be found as a sum over all quantum numbers of the FD distribution weighted by the energy of states.

$$E = \sum_{n_x} \sum_{n_y} \sum_{n_z} \epsilon f_+(\epsilon) \qquad (5)$$

Each quantum number can take any integer value greater than or equal to 1, so in principle, these sums extend to infinity. To analytically approach the problem, the summations are approximated with a continuous limit such that they are transformed into integrals. In this computational project, the sums are carried out without making a continuous approximation. Specifically, a relationship between the side length of the 3 dimensional box and the average energy of the system

can be found in terms of the container's volume and surface area and a small fluctuating term.

$$E = \rho_E V + \sigma_E A + \delta E \tag{6}$$

Dividing equation 6 through by L^2, the working equation of this project is obtained.

$$\frac{E}{L^2} = \rho_E L + 6\sigma_E + \frac{\delta E}{L^2} \tag{7}$$

Analytical values for the energy density of a Fermi gas are found in several introductory thermal physics and statistical mechanics textbooks (Kittel & Kroemer 1998) as

$$\frac{E}{V} = 0.6(\frac{N}{V})\epsilon_F \tag{8}$$

Where the Fermi energy ϵ_F is the energy of the highest occupied state for a system of Fermions at absolute 0. The Fermi energy can be found (Hoch 2021) to be

$$\epsilon_F = \frac{\hbar^2}{2m} \left(\frac{3\pi^2 N}{V} \right)^{2/3} \tag{9}$$

The surface energy in this model can also be derived following Stafford et al. (1999) as

$$\sigma_E = -\frac{\epsilon_F k_F^2}{16\pi} \tag{10}$$

where $k_F = \left(\frac{2m\epsilon_F}{\hbar^2}\right)^{1/2}$.

4. PROCEDURE

To set specific values for quantities such as the particle mass, I use values derived from an electron gas. The quantum electron gas is a well-studied physical scenario, which allows for comparison of final results with those found in previous literature.

Functions are defined to compute the energy of a quantum state given the quantum numbers and side length of the box and the FD distribution from these same parameters along with the chemical potential and thermodynamic beta. To carry out the summation to find the total system energy as a function of L, a further routine is defined which creates a range of side lengths and corresponding array of system energies. The system energy at each L value is determined by summing over all combinations of quantum numbers the energy of each state times the FD function. Because of limited computational resources, sums are terminated at a maximum integer value of 100 for each spacial quantum number. This limitation causes the computed data to deviate from the expected relationship between E and L outside for large L. Furthermore, extremely small values

for L only allow for a low number of particles, causing few-body effects to arise.

To account for these factors, the range of side lengths used in the calculation is first carried out over a large range to isolate the portion of the data which approximately follows the desired relationship. By visually inspecting a plot of E/L^2 against L, the working equation can be used. Because the energy density of a bulk Fermi gas must be positive, and since the fluctuating term δE is very small, one should expect to see the data approximate a line of positive slope within the region of interest. Once the relevant bounds are visually determined, the analysis is repeated within this smaller range. Then, using the curve_fit function from the SciPy Python package, a least-squares regression is carried out to fit the working equation to the data. This process directly yields in the best-fit parameters of interest. The analysis is repeated for three combinations of the thermodynamic beta and chemical potentials which represent a low, intermediate, and high temperature regime.

In addition to computing the system energy, a similar process is repeated in each case to determine the total particle number as a function of box side length. This is done by summing over twice the FD distribution over all quantum states. The particle number for each value of L is divided by L^3 to determine the particle number density. This density is averaged over all computed values within each temperature regime to account for small fluctuations. Using this density, the energy density and surface energy can be computed as a value for comparison with the results, as described in the Theory section.

Because each summation requires a number of steps equal to the maximum allowed spatial quantum number, and the three summations are nested to produce each combination of quantum numbers, the function to determine average system energy has a polynomial runtime of at least $\mathcal{O}(N^3)$. To allow for sufficiently high quantum numbers to be used in the calculation given the limited computing resources available, the Numba package is employed. This package is a Just-In-Time (JIT) compiler which converts and executes Python and NumPy code as machine code.

5. RESULTS

The average system energy was found as a function of box side length in three temperature regimes, and the system parameters were calculated for each. The results are summarized in Table 1. The analytical results calculated using the average particle density within each temperature regime are shown in Table 2.

Table 1. Energy density of Fermi gas (ρ_E), surface energy (σ_E), and fluctuation term (δE) at three temperature regimes

Temperature Regime	Temperature	$\beta\mu$	ρ_E	σ_E	δE
	K		$\frac{J}{m^3}$	$\frac{J}{m^2}$	J
Low	3	10	1.57×10^2	-5.61×10^{-7}	5.94×10^{-22}
Intermediate	300	1	3.12×10^5	-1.96×10^{-4}	8.36×10^{-21}
High	3000	0.1	4.66×10^7	-9.69×10^{-3}	4.37×10^{-20}

6. CONCLUSION

Examining the data generated, some significant trends are noted. As temperature increases, the energy density increases, the surface energy decreases, and the fluctuating term increases. The qualitative findings are in agreement with the those discussed in Stafford et al. (1997). The computationally derived values of the Fermi gas energy density and surface energy are within an order of magnitude of results obtained using the analytical methods. Noting the agreement between these two techniques, the numerical approach employed in this paper is shown to correctly predict the properties of a Fermi gas in a 3D box. In the future, these results could be expanded upon by investigating a greater variety of combinations of temperature and chemical potential, refining the computation by summing over a greater number of possible quantum states, or by expanding the investigation to consider a Bose gas. These satisfactory results using relatively simple statistical models allow for the characterization of complex phenomena ranging from free metals in a metallic lattice to the degeneracy pressure in a white dwarf star.

REFERENCES

Chandrasekhar, S. 1931, ApJ, 74, 81, doi: 10.1086/143324

Dyson, F. J., & Lenard, A. 1967, Journal of Mathematical Physics, 8, 423, doi: 10.1063/1.1705209

Fermi, E. 1926, Zeitschrift fur Physik, 36, 902, doi: 10.1007/BF01400221

Fowler, R. H. 1926, MNRAS, 87, 114, doi: 10.1093/mnras/87.2.114

Griffiths, D. J., & Schroeter, D. F. 2018, Introduction to quantum mechanics (Cambridge university press)

Hoch, M. J. 2021, Statistical and thermal physics: an introduction (CRC Press)

Kittel, C., & Kroemer, H. 1998, Thermal physics, American Association of Physics Teachers

Schulz, H. J. 1995, arXiv e-prints, cond, doi: 10.48550/arXiv.cond-mat/9503150

Sommerfeld, A. 1928, Zeitschrift fur Physik, 47, 1, doi: 10.1007/BF01391052

Stafford, C., Kassubek, F., Bürki, J., & Grabert, H. 1999, Physical Review Letters, 83, 4836

Stafford, C. A., Baeriswyl, D., & Bürki, J. 1997, PhRvL, 79, 2863, doi: 10.1103/PhysRevLett.79.2863

Stoner, E. C. 1930, The London, Edinburgh, and Dublin Philosophical Magazine and Journal of Science, 9, 944

Table 2. Analytically computed values of the energy density of Fermi gas (ρ_E) and surface energy (σ_E) at three temperature regimes. The same values of β and μ are used for each regime as in Table 1.

| Temperature Regime	Number Density	ϵ_F	ρ_E	σ_E
	m^{-3}	J	$\frac{J}{m^3}$	$\frac{J}{m^2}$
Low	5.49×10^23	3.92×10^{-22}	1.29×10^2	-5.00×10^{-7}
Intermediate	3.41×10^25	6.15×10^{-21}	1.26×10^5	-1.23×10^{-4}
High	6.01×10^26	4.16×10^{-20}	1.50×10^7	-5.65×10^{-3}
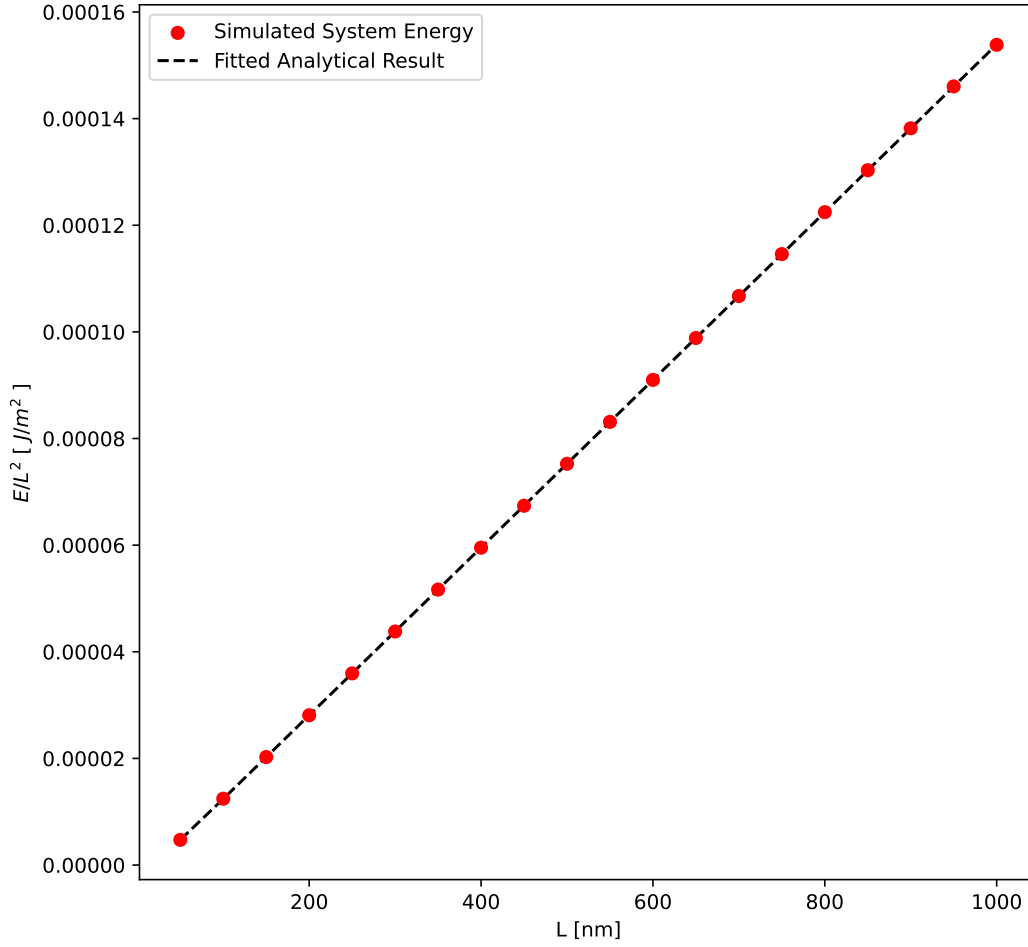
Figure 1. Average system energy over box side length squared vs side length for the low temperature regime. T = 3K and $\beta\mu = 10$. Parameters determined by fitting routine are shown in Table 1.
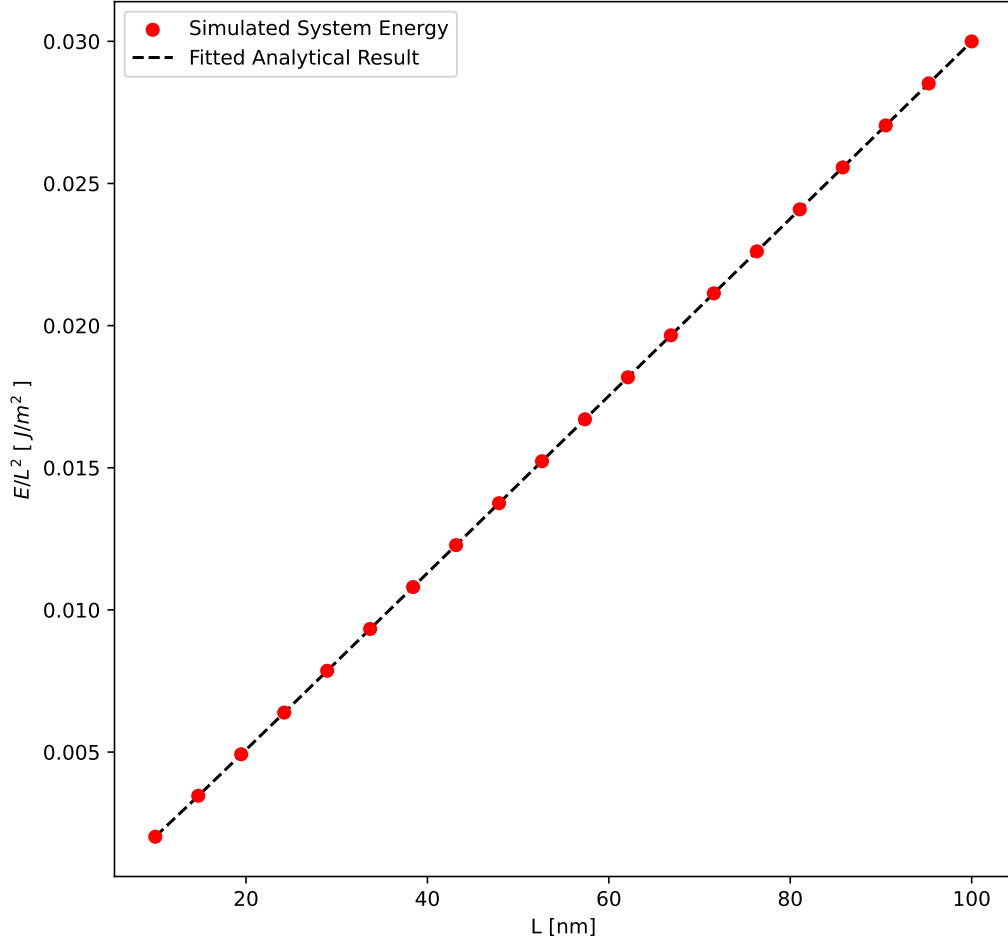
Figure 2. Average system energy over box side length squared vs side length for the low temperature regime. T = 300K and $\beta\mu = 1$. Parameters determined by fitting routine are shown in Table 1.
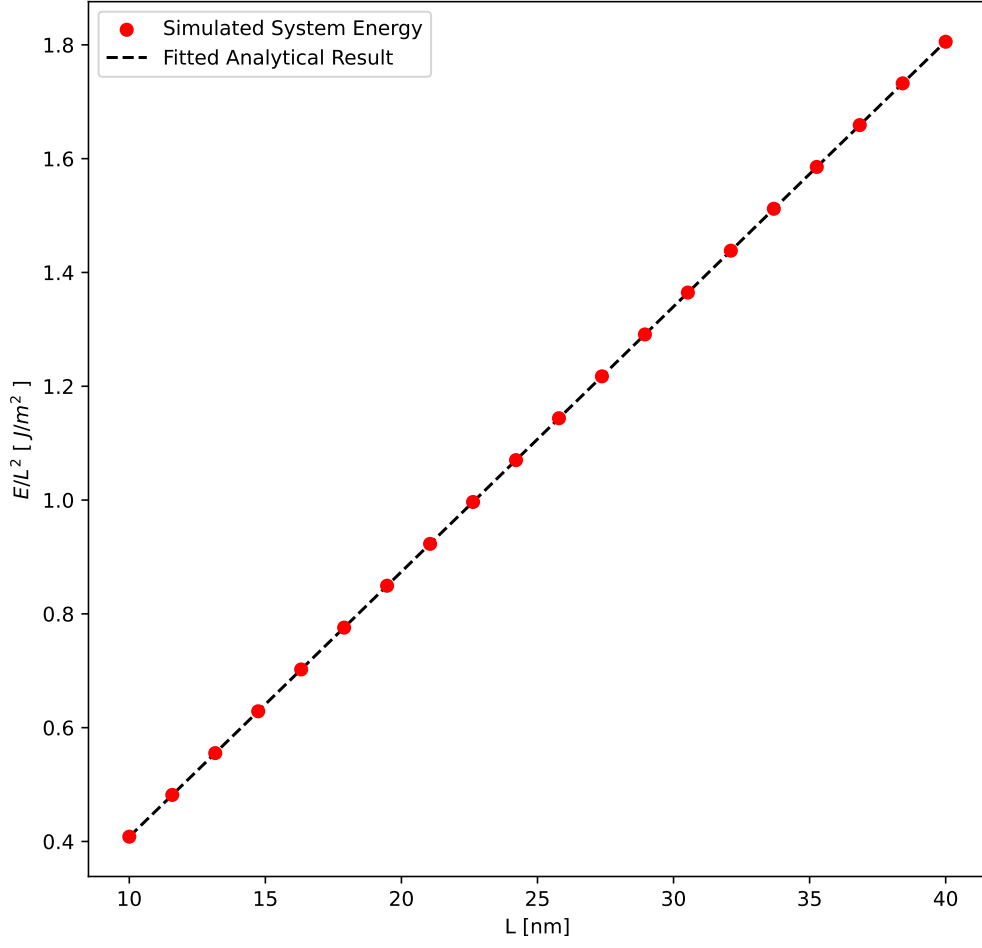
Figure 3. Average system energy over box side length squared vs side length for the low temperature regime. T = 3000K and $\beta\mu = 0.1$. Parameters determined by fitting routine are shown in Table 1.